

DHA: End-to-End Joint Optimization of Data Augmentation Policy, Hyper-parameter and Architecture

Kaichen Zhou,¹ Lanqing Hong,^{2*} Shoukang Hu,³ Fengwei Zhou,²
Binxin Ru,¹ Jiashi Feng,⁴ Zhenguo Li²

¹ University of Oxford, ² Huawei Noah’s Ark Lab, ³ The Chinese University of Hong Kong, ⁴ National University of Singapore

Abstract

Automated machine learning (AutoML) usually involves several crucial components, such as Data Augmentation (DA) policy, Hyper-Parameter Optimization (HPO), and Neural Architecture Search (NAS). Although many strategies have been developed for automating these components in separation, joint optimization of these components remains challenging due to the largely increased search dimension and the variant input types of each component. Meanwhile, conducting these components in a sequence often requires careful coordination by human experts and may lead to sub-optimal results. In parallel to this, the common practice of *searching* for the optimal architecture first and then *retraining* it before deployment in NAS often suffers from low performance correlation between the search and retraining stages. An end-to-end solution that integrates the AutoML components and returns a ready-to-use model at the end of the search is desirable. In view of these, we propose **DHA**, which achieves joint optimization of **D**ata augmentation policy, **H**yper-parameter and **A**rchitecture. Specifically, end-to-end NAS is achieved in a differentiable manner by optimizing a compressed lower-dimensional feature space, while DA policy and HPO are updated dynamically at the same time. Experiments show that DHA achieves state-of-the-art (SOTA) results on various datasets, especially 77.4% accuracy on ImageNet with cell based search space, which is higher than current SOTA by 0.5%. To the best of our knowledge, we are the first to efficiently and jointly optimize DA policy, NAS, and HPO in an end-to-end manner without retraining.

Introduction

While deep learning has achieved remarkable progress in various tasks such as computer vision and natural language processing, the design and training of a well-performing deep neural architecture for a specific task usually requires tremendous human involvement (He et al. 2016; Sandler et al. 2018). To alleviate such burden on human users, AutoML algorithms have been proposed in recent years to automate the pipeline of designing and training a model, such as automated Data Augmentation (DA), Hyper-Parameter Optimization (HPO), and Neural Architecture Search (NAS) (Cubuk et al. 2018; Mittal et al. 2020; Chen et al. 2019).

*honglanqing@huawei.com

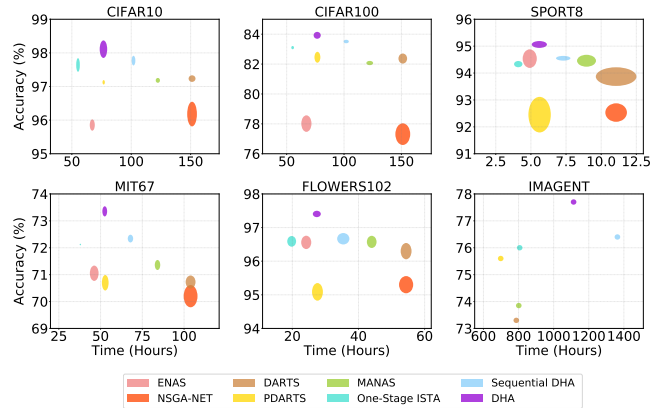


Figure 1: Top-1 accuracy and computational time of AutoML algorithms for classification task on various datasets, including CIFAR10, CIFAR100, SPORT8, MIT67, FLOWERS102 and ImageNet. Ellipse centres, ellipse edges represent the $\mu \pm \{0, \sigma/2\}$, respectively (mean μ , standard deviation σ). For ImageNet, we present test accuracy without error bars, as the error bars are not reported in the references.

All of these AutoML components are normally processed independently and the naive solution of applying them sequentially in separate stages, not only suffers from low efficiency but also leads to sub-optimal results (Dai et al. 2020; Dong et al. 2020). Indeed, how to achieve full-pipeline “from data to model” automation efficiently and effectively is still a challenging and open problem. One of the main difficulties lies in understanding how to automatically combine the different AutoML components (e.g., NAS and HPO) appropriately without human expertise. FBNetV3 (Dai et al. 2020) and AutoHAS (Dong et al. 2020) investigated the joint optimization of NAS and HPO, while (Kashima, Yamada, and Saito 2020) focused on the joint optimization of neural architectures and data augmentation policies. The joint optimization of NAS and quantization policy were also investigated in APQ (Wang et al. 2020). Clear benefits can be seen in the above works when optimizing two AutoML components together, which motivates the further investigation of “from data to model” automation. However, with the increasing number of AutoML components, the search space complexity is increased by several orders of magnitudes and it is challenging to operate in such a large search space. In addition, how these AutoML components affect each other

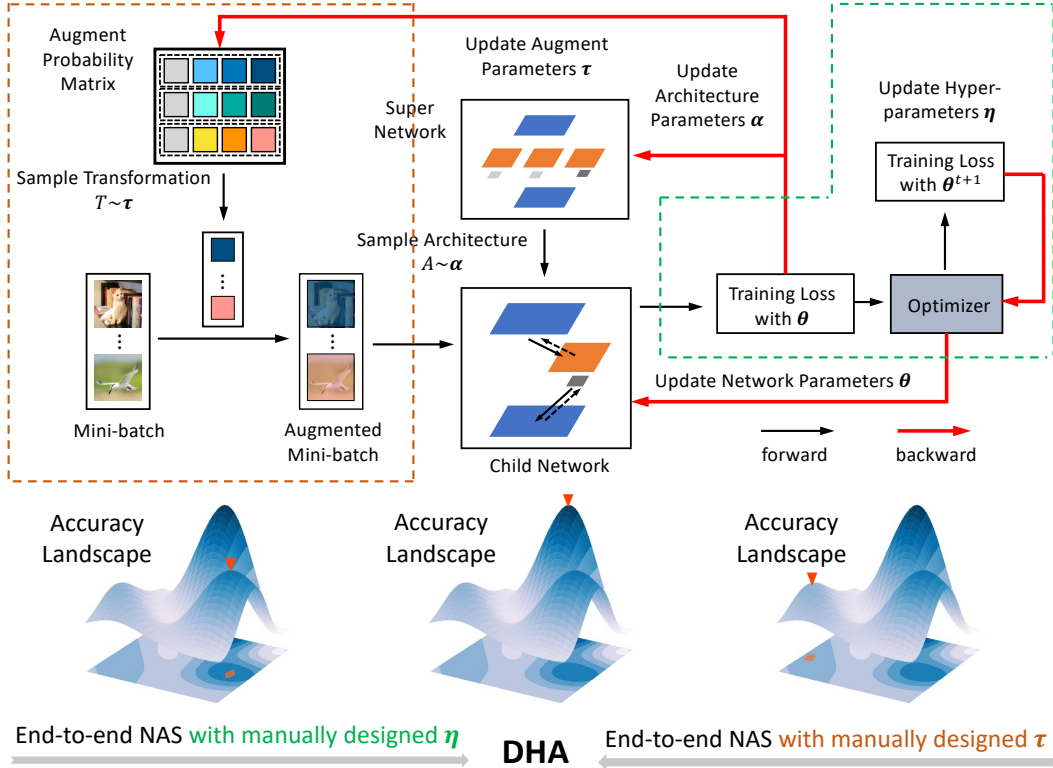


Figure 2: An overview of DHA. We first sample the DA operations for each sample based on the data transformation parameters τ . Then, a child network is sampled based on the architecture parameters α , which will be used to process the transformed mini-batch. Training loss is calculated to update the data transformation parameter τ , architecture parameters α , and neural network parameter θ . Then the training loss based on updated networks’ weights θ^{t+1} is used to update hyper-parameters η .

when optimized together is still unclear. Thus, further investigation is needed to open the black box of optimizing different AutoML components jointly.

Another main challenge of achieving the automated pipeline “from data to model” is understanding how to perform end-to-end searching and training of models without the need of parameter retraining. Current approaches, even those considering only one AutoML component such as NAS algorithms, usually require two stages, one for searching and one for retraining (Liu, Simonyan, and Yang 2019; Xie et al. 2019). Similarly, automatic DA methods such as FastAA (Lim et al. 2019) also need to retrain the model parameters once the DA policies have been searched. In these cases, whether the searched architectures or DA policies would perform well after retraining is questionable, due to the inevitable difference of training setup between the searching and retraining stages (Yang, Esperança, and Carlucci 2019). To improve the performance correlation between searching and retraining stages, DSNAS (Hu et al. 2020) developed a differentiable NAS method to provide direct NAS without parameter retraining. Other AutoML components, including HPO and automated DA, are seldom considered in the task-specific end-to-end AutoML algorithms.

Targeting the challenging task-specific end-to-end AutoML, we propose DHA, a differentiable joint optimization solution for efficient end-to-end AutoML components, including the DA, HPO and NAS. In DHA, the optimization strategy **weight-sharing** (Xie et al. 2020) is delicately

adopted in DA, HPO and NAS by respectively introducing the probability matrix, the continuous hyper-parameter setting and the super-network. Specifically, the DA and HPO are regarded as dynamic schedulers, which adapt themselves to the update of network parameters and network architecture. At the same time, the end-to-end NAS optimization is realized in a differentiable manner with the help of sparse coding method. Instead of performing our search in a high-dimensional network architecture space, we optimize a compressed lower-dimensional feature space. With this differentiable manner, DHA can effectively deal with the huge search space and the high optimization complexity caused by the joint optimization problem.

To summarize, our main contributions are as follows:

- We propose an AutoML method, DHA, for the concurrent optimization of DA, HPO and NAS. To the best of our knowledge, we are the first to efficiently and jointly optimize DA policy, HPO, and NAS in an end-to-end manner without retraining.
- Experiments show that DHA achieves a state-of-the-art (SOTA) 77.4% accuracy on ImageNet with cell based architecture search space. DHA also provides SOTA results on various datasets, including CIFAR10, CIFAR100, SPORT8, MIT67 and FLOWERS102 with relatively low computational cost, showing the effectiveness and efficiency of joint optimization (see Fig. 1).
- Thorough extensive experiments, we demonstrate the advantages of doing joint-training over optimizing each

AutoML component in sequence. Better model performance, higher efficiency and a smoother loss landscape are achieved by our proposed DHA method. Once the paper is accepted, we will release the code.

Related Works

Data augmentation. Learning data augmentation policies for a target dataset automatically has become a trend, considering the difficulty to elaborately design augmentation methods for various datasets (Cubuk et al. 2018; Zhang et al. 2020; Lin et al. 2019). Specifically, AutoAugment (Cubuk et al. 2018) and Adversarial AutoAugment (Zhang et al. 2020) adopt reinforcement learning to train a controller to generate policies, while OHL-Auto-Aug (Lin et al. 2019) formulates augmentation policy as a probability distribution and adopts REINFORCE (Williams 1992) to optimize the distribution parameters along with network training. PBA (Ho et al. 2019) and FAA (Lim et al. 2019) use population-based training method and Bayesian optimization respectively to reduce the computing cost of learning policies. (Cubuk et al. 2020) argues that the search space of policies used by these works can be reduced greatly and simple grid search can achieve competitive performance. They also point out that the optimal data augmentation policy depends on the model size, which indicates that fixing an augmentation policy when searching for neural architectures may lead to sub-optimal solutions.

Hyper-parameter optimization. Hyper-parameters also play an important role in the training paradigm of deep neural network models. Various black-box optimization approaches have been developed to address hyper-parameter tuning tasks involving multiple tasks (Mittal et al. 2020; Perrone et al. 2018) or mixed variable types (Ru et al. 2020). Meanwhile, techniques like multi-fidelity evaluations (Kandasamy et al. 2017; Wu et al. 2019), parallel computation (González et al. 2016; Kathuria, Deshpande, and Kohli 2016; Alvi et al. 2019), and transfer learning (Swersky, Snoek, and Adams 2013; Min, Gupta, and Ong 2020) are also employed to further enhance the query efficiency of the hyper-parameter optimization. In addition, several works (Bengio 2000; Lorraine, Vicol, and Duvenaud 2020; MacKay et al. 2019; Shaban et al. 2019; Maclaurin, Duvenaud, and Adams 2015) have proposed to use gradient-based bi-level optimization to tune large number of hyper-parameters during model training. Although many HPO strategies have been adopted in NAS strategies, methods that jointly optimize both architectures and hyper-parameters are rarely seen except the ones discussed below.

Neural architecture search. NAS has attracted growing attention over the recent years and provided architectures with better performance over those designed by human experts (e.g., Pham et al. 2018; Real et al. 2018; Liu, Simonyan, and Yang 2019). The rich collection of NAS literature can be divided into two categories: the query-based methods and the gradient-based ones. The former includes powerful optimization strategies such as reinforcement learning (Zoph and Le 2017; Pham et al. 2018), Bayesian optimization (Kandasamy et al. 2018; Ru, Esperanca, and Carlucci 2020) and evolutionary algorithms

(Elsken, Metzen, and Hutter 2019; Lu et al. 2019). The latter enables the use of gradients in updating both architecture parameters and network weights, which significantly reducing the computation costs of NAS via weight sharing (Liu, Simonyan, and Yang 2019; Chen et al. 2019; Xie et al. 2019; Hu et al. 2020). To reduce searching cost, most NAS methods search architectures in a low-fidelity set-up (e.g. fewer training epochs, smaller architectures) and retrain the optimal architecture using the full set-up before deployment. This separation of *search* and *evaluation* is sub-optimal (Hu et al. 2020), which motivates the development of end-to-end NAS strategies (Xie et al. 2019; Hu et al. 2020) that return read-to-deploy networks at the end of the search. Our work also proposes an end-to-end solution.

Joint optimization of AutoML components. Conventional neural architecture search methods perform a search over a fixed set of architecture candidates and then apply or search for a separate set of hyper-parameters when retraining the best architecture derived from the architecture search phase. Such search protocol may lead to sub-optimal results (Zela et al. 2018; Dong et al. 2020) as it neglects the influence of training hyper-parameters on architecture performance and ignores superior architectures under alternative hyper-parameter values (Dai et al. 2020). Given this, several works have been proposed to jointly optimize architecture structure and training hyper-parameters (Dai et al. 2020; Wang et al. 2020; Dong et al. 2020). Zela et al. (2018) introduces the use of multi-fidelity Bayesian optimization to search over both the architecture structure and training hyper-parameters. Dai et al. (2020) trains an accuracy predictor to estimate the network performance based on both the architecture and training hyper-parameters and then uses an evolutionary algorithm to perform the search. Both these methods are query-based and require a relatively large number of architecture and hyper-parameter evaluations to fine-tune predictors or obtain good recommendations. To improve the joint optimization efficiency, AutoHAS (Dong et al. 2020) introduces a differentiable approach in conjunction with weight sharing for the joint optimization task, which empirically demonstrates that such a differentiable one-shot approach achieves superior efficiency over query-based methods. In addition to jointly optimizing neural architectures and hyper-parameters, the other line of research focuses on the joint optimization of neural architectures and data augmentation hyper-parameters (Kashima, Yamada, and Saito 2020). Our proposed method differs from the above works in mainly two aspects: first, our method is more efficient than AutoHAS since our method has no need to update the whole network and only needs to update the sampled sub-network at each optimization step. Second, the joint optimization scope is further extended from NAS and training hyper-parameters to include DA, HPO and NAS.

Methodology

Consider a dataset $\mathcal{D} = \{(x_i, y_i)\}_{i=1}^N$, where N is the size of this dataset, and y_i is the label of the input sample x_i . We aim to train a neural network $f(\cdot)$, which can achieve the best accuracy on the test dataset \mathcal{D}^{test} . Multiple AutoML components are considered, including DA, HPO, and NAS.

Let τ , η , α , and θ represent the data augmentation parameters, the hyper-parameters, the architecture parameters, and the objective neural network parameters, respectively. This problem can be formulated as

$$\begin{aligned} & \operatorname{argmin}_{\tau, \eta, \alpha, \theta} \mathcal{L}(\tau, \eta, \alpha, \theta; \mathcal{D}) \\ \text{s.t. } & c_i(\alpha) \leq C_i, i = 1, \dots, \gamma, \end{aligned} \quad (1)$$

where $\mathcal{L}(\cdot)$ represents the loss function, \mathcal{D} denotes the input data, $c_i(\cdot)$ refers to the resource cost (e.g., storage or computational cost) of the current architecture α , which is restricted by the i -th resource constraints C_i , and γ denotes the total number of resource constraints. Considering the huge search space, it is challenging to achieve the joint optimization of τ , η , α , and θ within one-stage without parameter retraining. In this work, we propose to use the differentiable method to provide a computationally efficient solution. See Fig. 2 for an illustration.

Data augmentation parameters

For every mini-batch of training data $\mathcal{B}^{tr} = \{(x_k, y_k)\}_{k=1}^{n^{tr}}$ with batch size n^{tr} , we conduct data augmentation to increase the diversity of the training data. We consider K data augmentation operations, and each training sample is augmented by a transformation consisting of two successive operations (Cubuk et al. 2018; Lim et al. 2019). Each operation is associated with a magnitude that is uniformly sampled from $[0, 10]$. The data augmentation parameter τ represents a probability distribution over the augmentation transformations. For t -th iteration, we sample n^{tr} transformations according to τ^t with Gumbel-Softmax reparameterization (Maddison, Mnih, and Teh 2016) and to generate the corresponding augmented samples in the batch. Given a sampled architecture, the loss function for each augmented sample is denoted by $\mathcal{L}^{tr}(f(\alpha^t, \theta^t; \mathcal{T}_k(x_k)))$, where \mathcal{T}_k represents the selected transformation. In order to relax τ to be differentiable, we regard $p_k(\tau^t)$, the probability of sampling the transformation \mathcal{T}_k , as an importance weight for the loss function of corresponding sample $\mathcal{L}^{tr}(f(\alpha^t, \theta^t; \mathcal{T}_k(x_k)))$. The objective of data augmentation is to minimize the following loss function:

$$\mathcal{L}^{DA}(\tau^t) = - \sum_{k=1}^{n^{tr}} p_k(\tau^t) \mathcal{L}^{tr}(f(\alpha^t, \theta^t; \mathcal{T}_k(x_k))). \quad (2)$$

With this loss function, DHA intends to increase the sampling probability of those transformations that can generate samples with high **training loss**. By sampling such transformations, DHA can pay more attention to more aggressive DA strategies and increase model robustness against difficult samples (Zhang et al. 2020). However, blindly increasing the difficulty of samples may cause the **augment ambiguity** phenomenon (Wei et al. 2020): augmented images may be far away from the majority of clean images, which could cause the under-fitting of model and deteriorate the learning process. Hence, besides optimizing the probability matrix of DA strategies, we randomly sample the magnitude of each chosen strategy from an **uniform distribution**, which can prevent learning heavy DA strategies: augmenting

samples with large magnitude strategies. Moreover, instead of training a controller to generate adversarial augmentation policies via reinforcement learning (Zhang et al. 2020) or training an extra teacher model to generate additional labels for augmented samples (Wei et al. 2020), we search for the probability distribution of augmentation transformations directly via gradient-based optimization. In this way, the optimization of data augmentation is very efficient and hardly increases the computing cost.

Hyper-parameters

As shown in Fig. 2, given the batch of augmented training data $\{(\mathcal{T}_k(x_k), y_k)\}_{k=1}^{n^{tr}}$ and the sampled child network, we need to optimize the differentiable hyper-parameters η , such as learning rate and L2 regularization. At the training stage, we alternatively update θ and η . In t -th iteration, we can update θ^t based on the gradient of the unweighted training loss $\mathcal{L}^{tr}(f(\alpha^t, \theta^t; \mathcal{B}^{tr})) = \frac{1}{n^{tr}} \sum_{k=1}^{n^{tr}} \mathcal{L}^{tr}(f(\alpha^t, \theta^t; \mathcal{T}_k(x_k)))$, which can be written as:

$$\theta^{t+1} = OP(\theta^t, \eta^t, \nabla_{\theta} \mathcal{L}^{tr}(f(\alpha^t, \theta^t; \mathcal{B}^{tr}))), \quad (3)$$

where $OP(\cdot)$ is the optimizer. To update the hyper-parameters η , we regard θ^{t+1} as a function of η and compute the **training loss** $\mathcal{L}^{tr}(f(\alpha^t, \theta^{t+1}(\eta^t); \mathcal{B}^{tr}))$ with network parameters $\theta^{t+1}(\eta^t)$ on a mini-batch of training data \mathcal{B}^{tr} . Then, η^t is updated with $\nabla_{\eta} \mathcal{L}^{tr}(f(\alpha^t, \theta^{t+1}(\eta^t); \mathcal{B}^{tr}))$ by gradient descent:

$$\eta^{t+1} = \eta^t - \beta \nabla_{\eta} \mathcal{L}^{tr}(f(\alpha^t, \theta^{t+1}(\eta^t); \mathcal{B}^{tr})), \quad (4)$$

where β is a learning rate. Even θ^t can also be deployed to θ^{t-1} whose calculation also involves η^{t-1} , we take an approximation method in Eqn. (4) and regard θ^t here as a variable independent of η^{t-1} . Instead of splitting an extra validation set for HPO, we directly sample a subset from training set to update η , which could ensure that the whole training set is used in updating τ , η , α , and θ .

Architecture parameters

With the augmented data in previous section, we achieve the optimization of the architecture parameter α through end-to-end NAS, motivated by SNAS (Xie et al. 2019), DSNAS (Hu et al. 2020) and ISTA-NAS (Yang et al. 2020). Following Liu, Simonyan, and Yang (2019), we denote the each space as a single directed acyclic graph (DAG), where the probability matrix α consists of vector $\alpha_{i,j}^T = [\alpha_{i,j}^1, \dots, \alpha_{i,j}^r, \dots, \alpha_{i,j}^k]$ and $\alpha_{i,j}^r$ represents the probability of choosing r^{th} operation associated with the edge (i, j) . Instead of directly optimizing $\alpha \in \mathbb{R}^n$, we adopt ISTA-NAS to optimize its compressed representation $\mathbf{b} \in \mathbb{R}^m$ where $m \ll n$, which can be written as:

$$\mathbf{b} = \mathbf{A}\alpha + \epsilon, \quad (5)$$

where $\epsilon \in \mathbb{R}^m$ represents the noise and $\mathbf{A} \in \mathbb{R}^{m \times n}$ is the measurement matrix which is randomly initialized. Eqn. (5) is solved through using LASSO loss function (Tibshirani 1996) and the α is optimized by using iterative shrinkage

thresholding algorithm (Daubechies, Defrise, and De Mol 2004), which can be written as:

$$\alpha^{t+1} = \eta_{\lambda/L}(\alpha^t - \frac{1}{L} \mathbf{A}^T(\mathbf{A}\alpha - \mathbf{b})), t = 0, 1, \dots, \quad (6)$$

where L represents the LASSO formulation which can be written as $\min_{\alpha} \frac{1}{2} \|\mathbf{A}\alpha - \mathbf{b}\|_2^2 + \lambda \|\alpha\|_1$; the λ represents the regularization parameters and the $\eta_{\lambda/L}$ is the shrinkage operator as defined in (Beck and Teboulle 2009). Thus we have:

$$\alpha_j^T \mathbf{o}_j = (\mathbf{b}_j^T \mathbf{A}_j - [\alpha_j(\mathbf{b}_j)]^T \mathbf{E}_j) \mathbf{o}_j, \quad (7)$$

where \mathbf{o}_j refer to all possible operations connected to note j and $\mathbf{E}_j = \mathbf{A}_j^T \mathbf{A}_j - \mathbf{I}$. With this relaxation, \mathbf{b} can be optimized through calculating the gradient concerning **training loss**. The main reason for using this optimization algorithm is that it can optimize the high-dimensional architecture parameters through optimizing low-dimensional embeddings, which can largely decrease the optimization difficulty and increase the optimization efficiency. Moreover, this algorithm also adopt the weights sharing in the optimization process which can be readily combined with our proposed data augmentation and hyper-parameter optimization method.

Joint-optimization

Based on the above analysis of each AutoML module, DHA realizes end-to-end joint optimization of automated data augmentation parameters τ , hyper-parameters η , and architecture parameters α . The DHA algorithm is summarized in Algorithm 1. One-level optimization is applied to τ and α as in Line 6 and, Line 6 and Line 8, while bi-level optimization is applied to η as in Line 9. **One thing worth mentioning is that different optimizers are adopted for different parameters.** There are two main reasons behind this choice. Firstly, τ , η , α and θ work differently in the optimization process, e.g., τ controls the transformation strategy for the training set while α is related to the architecture selection. Besides θ , other parameters couldn't directly be optimized through the gradient descent on training set. These differences cause the different optimization methods for τ , α , η and θ . Secondly, τ , α , η and θ have different dimensions and different scales, which makes the joint-optimization with a uniform optimizer extremely impracticable. This is why current works concerning DA (Ho et al. 2019), NAS (Yao et al. 2020; Nekrasov et al. 2019) and HPO (Falkner, Klein, and Hutter 2018) always adopt different optimizer for network's weights and hyper-parameters they aim to optimize. Moreover, the main reason that DHA could optimize large-scale search space in an effectively manner, is that DHA delicately adopt **weight-sharing** in the joint-optimization for different parameters. Instead of only optimizing a sub-network with a DA strategy and a hyper-parameter setting to check the performance of certain setting, we realize the joint-optimization with the help of a super-net network, a DA probability matrix and continuous hyper-parameter setting. In that way, DHA can make use of previous trained parameter weights to check the performance setting, which largely decreases the computational request.

Algorithm 1: DHA

Initialization: Data Transformation Parameters τ , Hyper-parameters η , Compressed Representation \mathbf{b} , Measurement Matrix \mathbf{A} , and Network Parameters θ

Input: Training Set \mathcal{D}^{tr} , Parameters τ , η , \mathbf{b} , \mathbf{A} , θ , and the iteration number T

Return: τ , η , α , θ

- 1: **while** $t < T$ **do**
 - 2: Separately sample a mini-batch \mathcal{B}^{tr} from \mathcal{D}^{tr} ;
 - 3: For each sample x_k in mini-batch \mathcal{B}^{tr} , sample a transformation $\mathcal{T}_k(x_k)$ according to τ^t ;
 - 4: Recover α^t by solving Eqn. 5 with \mathbf{b}^t and \mathbf{A} ;
 - 5: Extract a child network from the super network;
 - 6: Compute the weighted training loss function as Eqn. (2) and update τ^{t+1} accordingly;
 - 7: Calculate θ^{t+1} with Eqn. (3);
 - 8: Use training loss function to update \mathbf{b}^{t+1} through the gradient descent, then α^{t+1} is updated with Eqn. (6);
 - 9: Compute the training loss function with θ^{t+1} on \mathcal{D}^{val} and update η^{t+1} with Eqn. (4);
 - 10: **end while**
-

Experiments

In this section, we empirically compare DHA against existing AutoML algorithms on various datasets. With extensive experiments, we demonstrate the benefits of joint-optimization over sequential-optimization in terms of generalization performance and computational efficiency.

Experiment setting

Datasets. Following Ru, Esperanca, and Carlucci (2020), we conducted experiments on various datasets, including CIFAR10 and CIFAR100 for the object classification task (Krizhevsky, Hinton et al. 2009), SPORT8 for the action classification task (Li and Fei-Fei 2007), MIT67 for the scene classification task (Quattoni and Torralba 2009), FLOWERS102 for the fine object classification task (Nilsback and Zisserman 2008), and ImageNet(Russakovsky et al. 2015) for the large-scale classification task. The accuracy is calculated on the test set.

Search space. (1) Automated DA. Following Ho et al. (2019), we consider 14 different operations for data augmentation, such as AutoContrast and Equalize. The magnitude of each operation is randomly sampled from the uniform distribution. **(2) NAS.** Following Liu, Simonyan, and Yang (2019), we consider the cell-based search space, which regards the whole architecture as a stack similar cells. **(3) HPO.** We consider both the L2 regularization (i.e., weight decay) and the learning rate in the experiments. Detailed search spaces are provided in Appendix.

Baselines. We compare DHA with various AutoML algorithms (see Table 1 and Table 2). For datasets including CIFAR10, CIFAR100, SPORT8, MIT67 and FLOWERS102, we re-implement existing works following the papers cited in Table 1 (see Appendix for more details). As for ImageNet, we directly refer to the model performance reported in papers cited in Table 2. To further demonstrate the benefits

Table 1: Top-1 accuracy (%) and computational time (GPU hour) of different AutoML algorithms on CIFAR10, CIFAR100, SPORT8, MIT67 and FLOWERS102. We report the sum of search time and tune time for two-stage NAS and the whole running time for one-stage NAS. All the methods are implemented by ourselves. Different NAS algorithms for one dataset are performed under the similar parameter weights constrain to ensure fair comparison.

Model	CIFAR10		CIFAR100		SPORT8		MIT67		FLOWERS102	
	Acc	Time	Acc	Time	Acc	Time	Acc	Time	Acc	Time
ENAS (Pham et al. 2018)	95.85±0.17	67.20	78.02±0.55	67.20	94.54±0.35	4.90	71.05±0.29	46.20	96.56±0.20	24.20
NSGA-NET (Lu et al. 2019)	96.18±0.37	151.20	77.31±0.14	151.20	92.53±0.34	11.10	70.20±0.41	103.90	95.30±0.26	54.40
DARTS (Liu, Simonyan, and Yang 2019)	97.24±0.10	151.20	82.37±0.34	151.20	93.87±0.35	11.10	70.73±0.24	103.90	96.30±0.24	54.40
P-DARTS (Chen et al. 2019)	97.13±0.07	76.80	82.46±0.37	76.80	92.45±0.66	5.60	70.70±0.29	52.80	95.09±0.26	27.60
MANAS (Carlucci et al. 2019)	97.18±0.07	122.40	82.07±0.14	122.40	94.46±0.22	8.90	71.36±0.19	84.10	96.57±0.18	44.00
One-Stage ISTA (Yang et al. 2020)	97.64±0.20	55.20	83.10±0.11	55.20	94.33±0.12	4.10	72.12±0.03	37.90	96.59±0.16	19.80
Sequential DHA	97.77±0.14	101.90	83.51±0.12	101.90	94.55±0.09	7.30	72.34±0.14	67.90	96.67±0.17	35.40
DHA	98.11±0.26	76.60	83.93±0.23	76.60	95.06±0.13	5.60	73.35±0.19	52.50	97.41±0.09	27.40

of joint optimization of multiple AutoML components, we also include a baseline, **Sequential DHA**, which resembles the common practice by human to optimize different components in sequence. Specifically, Sequential DHA consists of two stages. During the first stage, Sequential DHA performs NAS to find the optimal architecture under certain hyper-parameter settings. In the next stage, Sequential DHA performs the online DA and HPO strategy proposed in our paper and trains the architecture derived from the first stage from scratch. These experiments are conducted on NVIDIA V100 under PyTorch-1.3.0 and Python 3.6. Detailed settings of baselines are provided in Appendix.

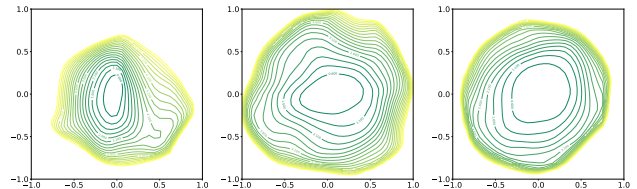
Results

The test accuracy and computational time of various AutoML algorithms are summarized in Table 1 and Table 2. The timing results in these two tables measure the computational time taken to obtain a ready-to-deploy network, which corresponds to the sum of search and retrain time for two-stage NAS methods and the search time for end-to-end methods like one-stage NAS method as well as our DHA. As shown in Table 1, methods optimising all of DA, HPO and NAS automatically (i.e, Sequential DHA and DHA) consistently outperform those NAS algorithms with manual designed DA and HPO. Specifically, DHA achieves SOTA results on all datasets. This shows the clear performance gain of extending the search scope from architecture to including also data augmentation and hyper-parameters, justifying the need for multi-component optimization in AutoML. Moreover, despite optimising over a larger search space, DHA remains cost efficiency. For example, on CIFAR100, DHA enjoys 1.56% higher test accuracy than DARTS but requires 42% less time. Besides, the comparison between DHA and Sequential DHA reveals the evident advantage of doing DA, HPO and NAS jointly over doing them separately in different stages. The Top-1 accuracy and computation time of these AutoML algorithms are also summarized in Fig. 1. As can be seen, DHA consistently gains highest test accuracy on all five datasets while being more cost efficient than NAS methods and Sequential DHA.

Results of the large-scale dataset ImageNet are shown in Table 2. DHA consistently outperforms various NAS methods which only involves architecture optimization, demonstrating the benefits of joint-optimization. Even when

compared with One-stage NAS methods like ISTA, DHA achieves up to 1.7% TOP-1 accuracy improvement. Moreover, in comparison with the joint-optimization algorithm APQ (Wang et al. 2020), DHA outperforms APQ by 2.5% and only takes 54% time. These comparisons reveal that DHA proposes an efficient and high-performed joint-optimization algorithm.

Analysis of loss landscape



(a) One-Stage ISTA (b) Sequential DHA (c) DHA
Figure 3: Loss-landscape of the trained models on SPORT8.
(a) One-Stage ISTA (b) Sequential DHA and (c) DHA.

The strong test performance of DHA across various datasets motivates us to further check the geometry of the minimiser achieved by our final trained model. We employ the filter-normalisation method proposed in Li et al. (2017) to visualise the local loss landscape around the minimiser achieved by One-Stage ISTA, Sequential DHA and DHA. We choose a center point θ^* in the graph, and two direction vector δ and η . We the plot the 2D contour with the function $f(\alpha, \beta) = \mathcal{L}(f(\theta^* + \alpha\delta + \beta\eta; \mathcal{B}^{test}))$, where \mathcal{B}^{test} represents the test set. The resultant contour plots are shown in Fig. 3. As can be seen, the minimum reached by optimising over more AutoML components tend to be flatter than NAS with manual designed DA and HPO. The loss landscape of DHA is also flatter and smoother than that of Sequential DHA accounting for the better generalisation performance of DHA in previous experiments, explaining the superior test accuracy achieved by DHA in Tables 1 and 2 (Keskar et al. 2016; Xu and Mannor 2012).

Ablation study of AutoML components

To further verify the effectiveness of our proposed extended search scope and search strategy, we empirically investigate the performance of considering all three components (i.e., DA, HPO and NAS) against combining any two of them. We examine both the sequential-optimization and

Table 2: Comparison with SOTA image classifiers on ImageNet in the Mobile setting. ([†] denotes the architecture is searched on ImageNet, otherwise it is searched on CIFAR-10 or CIFAR-100.)

Model	Test Acc (%)		Params (M)	Cost (GPU-day)		Search Attribute
	Top-1	Top-5		Search	Eval	
DARTS (2nd) (Liu, Simonyan, and Yang 2019)	73.3	91.3	4.7	4.0	3.6×8	Arch
SNAS (mild) (Xie et al. 2019)	72.7	90.8	4.3	1.5	3.3×8	Arch
GDAS (Dong and Yang 2019)	74.0	91.5	5.3	0.3	3.6×8	Arch
BayesNAS (Zhou et al. 2019)	73.5	91.1	3.9	0.2	3.6×8	Arch
PARSEC (Casale, Gordon, and Fusi 2019)	74.0	91.6	5.6	1.0	3.6×8	Arch
P-DARTS (CIFAR-10) (Chen et al. 2019)	75.6	92.6	4.9	0.3	3.6×8	Arch
P-DARTS (CIFAR-100) (Chen et al. 2019)	75.3	92.5	5.1	0.3	3.6×8	Arch
EfficientNet-B0 (Tan and Le 2019) [†]	77.1	93.3	5.3	-	-	Arch
SinglePathNAS (Guo et al. 2019) [†]	74.7	-	3.4	13.0	2.0×8	Arch
ProxylessNAS (GPU) (Cai, Zhu, and Han 2019) [†]	75.1	92.5	7.1	8.3	3.6×8	Arch
PC-DARTS (ImageNet) (Xu et al. 2020) [†]	75.8	92.7	5.3	3.8	3.9×8	Arch
GAEA+PC-DARTS (Li et al. 2021) [†]	76.0	92.7	5.6	3.8	3.9×8	Arch
DrNAS (Chen et al. 2021) [†]	76.3	92.9	5.7	4.6	3.9×8	Arch
DSNAS (Hu et al. 2020) [†]	74.3	91.9	-	3.7×8	-	Arch
One-Stage ISTA (Yang et al. 2020) [†]	76.0	92.9	5.7	4.2×8	-	Arch
OFA (small) (Cai et al. 2020) [†]	76.9	93.3	5.8	6.8×8	-	Arch + Resolution
APQ (Wang et al. 2020) [†]	75.1	-	-	12.5×8	-	Arch + Pruning + Quant Policy
Sequential DHA [†]	76.7	93.8	5.4	1.6×8	5.5×8	Arch + Data Aug + Hyper-param
DHA [†]	77.4	94.6	5.6	5.8×8	-	

Table 3: Top-1 accuracy (%) and computational time (GPU hour) of different combination of AutoML components on CIFAR10, CIFAR100, SPORT8, MIT67 and FLOWERS102. Listed algorithms are described in Ablation study.

Model	CIFAR10		CIFAR100		SPORT8		MIT67		FLOWERS102	
	Acc	Time	Acc	Time	Acc	Time	Acc	Time	Acc	Time
Sequential NAS+DA	97.74±0.12	57.50	83.45±0.03	57.50	94.49±0.03	4.20	72.22±0.04	39.20	96.64±0.03	20.50
Sequential NAS+HPO	97.54±0.18	63.60	83.13±0.05	63.60	94.47±0.04	4.60	72.10±0.05	43.10	96.57±0.02	22.50
Sequential DHA	97.77±0.14	101.90	83.51±0.12	101.90	94.55±0.09	7.30	72.34±0.14	67.90	96.67±0.17	35.40
Joint-optimization NAS+DA	97.78±0.13	64.00	83.55±0.03	64.00	94.53±0.09	4.70	72.38±0.19	43.80	96.72±0.01	22.90
Joint-optimization NAS+HPO	97.75±0.20	70.80	83.23±0.05	70.80	94.50±0.08	5.20	72.23±0.12	47.80	96.69±0.08	25.40
DHA	98.11±0.26	76.60	83.93±0.23	76.60	95.06±0.13	5.60	73.35±0.19	52.50	97.41±0.22	27.40

joint-optimization settings with four designed optimization algorithms. **Sequential NAS + DA** first conducts NAS and during the tuning stage, the proposed DA optimization is applied. Similar to the Sequential NAS+DA, **Sequential NAS + HPO** firstly conducts NAS. Then with the fixed architecture, Sequential NAS + DA optimizes the HPO and networks’ weights simultaneously. In contrast to them, **Joint-optimization NAS + DA** simultaneously conducts DA strategy optimization, NAS and parameter weights optimization. **Joint-optimization NAS + HPO** simultaneously conducts HPO, NAS and parameter weights optimization.

The comparison results are presented in Table 3. We can notice that performing joint optimization for either NAS + DA or NAS + HPO, achieves higher test accuracy than doing them in a pipeline. This reconfirms our previous conclusion that optimising different AutoML components jointly is better than doing them in sequence. Moreover, by comparing the results of the joint-optimization NAS+DA and the joint-optimization NAS+HPO in Table 3 against the One-Stage ISTA in Table 1, it is clear that considering one more AutoML component on top of NAS can lead to clear per-

formance gain of the final model. While such gain is higher for incorporating DA than HPO, it is maximised when all three components are considered; our DHA obtains the best test accuracy among all joint-optimization baselines across all datasets.

Conclusion

In this work, we present DHA, an end-to-end joint-optimization method for three important components of AutoML, including DA, HPO and NAS. This differentiable joint-optimization method can efficiently optimize larger search space than precious AutoML methods and achieve SOTA results on various datasets with a relatively low computational cost. Specifically, DHA achieves 77.4% Top-1 accuracy on ImageNet with cell based search space, which is higher than current SOTA by 0.5%. With DHA, we show the advantage of doing joint-optimization of AutoML over doing co-optimization in sequence, and conclude that joint optimization of multiple AutoML components is necessary.

References

- Alvi, A. S.; Ru, B. X.; Calliess, J.-P.; Roberts, S. J.; and Osborne, M. A. 2019. Asynchronous batch Bayesian optimisation with improved local penalisation. In *ICML*.
- Beck, A.; and Teboulle, M. 2009. A fast iterative shrinkage-thresholding algorithm for linear inverse problems. *SIAM journal on imaging sciences*, 2(1): 183–202.
- Bengio, Y. 2000. Gradient-based optimization of hyperparameters. *Neural Computation*, 12(8): 1889–1900.
- Cai, H.; Gan, C.; Wang, T.; Zhang, Z.; and Han, S. 2020. Once-for-all: Train one network and specialize it for efficient deployment. In *ICLR*.
- Cai, H.; Zhu, L.; and Han, S. 2019. Proxylessnas: Direct neural architecture search on target task and hardware. In *ICLR*.
- Carlucci, F. M.; Esperança, P. M.; Singh, M.; Gabillon, V.; Yang, A.; Xu, H.; Chen, Z.; and Wang, J. 2019. MANAS: Multi-agent neural architecture search. *arXiv preprint arXiv:1909.01051*.
- Casale, F. P.; Gordon, J.; and Fusi, N. 2019. Probabilistic neural architecture search. *arXiv preprint arXiv:1902.05116*.
- Chen, X.; Wang, R.; Cheng, M.; Tang, X.; and Hsieh, C.-J. 2021. DrNAS: Dirichlet neural architecture search. In *ICLR*.
- Chen, X.; Xie, L.; Wu, J.; and Tian, Q. 2019. Progressive differentiable architecture search: Bridging the depth gap between search and evaluation. In *CVPR*.
- Cubuk, E. D.; Zoph, B.; Mane, D.; Vasudevan, V.; and Le, Q. V. 2018. AutoAugment: Learning augmentation policies from data. *arXiv preprint arXiv:1805.09501*.
- Cubuk, E. D.; Zoph, B.; Shlens, J.; and Le, Q. V. 2020. RandAugment: practical automated data augmentation with a reduced search space. In *CVPR Workshops*.
- Dai, X.; Wan, A.; Zhang, P.; Wu, B.; He, Z.; Wei, Z.; Chen, K.; Tian, Y.; Yu, M.; Vajda, P.; et al. 2020. FBNetV3: Joint architecture-recipe search using neural acquisition function. In *CVPR*.
- Daubechies, I.; Defrise, M.; and De Mol, C. 2004. An iterative thresholding algorithm for linear inverse problems with a sparsity constraint. *Communications on Pure and Applied Mathematics: A Journal Issued by the Courant Institute of Mathematical Sciences*, 57(11): 1413–1457.
- Dong, X.; Tan, M.; Yu, A. W.; Peng, D.; Gabrys, B.; and Le, Q. V. 2020. AutoHAS: Differentiable hyper-parameter and architecture search. *arXiv preprint arXiv:2006.03656*.
- Dong, X.; and Yang, Y. 2019. Searching for a robust neural architecture in four GPU hours. In *CVPR*.
- Elsken, T.; Metzen, J. H.; and Hutter, F. 2019. Efficient multi-objective neural architecture search via Lamarckian evolution. In *ICLR*.
- Falkner, S.; Klein, A.; and Hutter, F. 2018. BOHB: Robust and efficient hyperparameter optimization at scale. In *ICML*.
- González, J.; Dai, Z.; Hennig, P.; and Lawrence, N. D. 2016. Batch Bayesian optimization via local penalization. In *International Conference on Artificial Intelligence and Statistics*.
- Guo, Z.; Zhang, X.; Mu, H.; Heng, W.; Liu, Z.; Wei, Y.; and Sun, J. 2019. Single path one-shot neural architecture search with uniform sampling. *arXiv preprint arXiv:1904.00420*.
- He, K.; Zhang, X.; Ren, S.; and Sun, J. 2016. Deep residual learning for image recognition. In *CVPR*.
- Ho, D.; Liang, E.; Chen, X.; Stoica, I.; and Abbeel, P. 2019. Population based augmentation: Efficient learning of augmentation policy schedules. In *ICML*.
- Hu, S.; Xie, S.; Zheng, H.; Liu, C.; Shi, J.; Liu, X.; and Lin, D. 2020. DSNAS: Direct neural architecture search without parameter retraining. In *CVPR*.
- Kandasamy, K.; Dasarathy, G.; Schneider, J.; and Póczos, B. 2017. Multi-fidelity Bayesian optimisation with continuous approximations. In *ICML*.
- Kandasamy, K.; Neiswanger, W.; Schneider, J.; Póczos, B.; and Xing, E. P. 2018. Neural architecture search with Bayesian optimisation and optimal transport. In *NeurIPS*.
- Kashima, T.; Yamada, Y.; and Saito, S. 2020. Joint search of data augmentation policies and network architectures. In *CoRR*.
- Kathuria, T.; Deshpande, A.; and Kohli, P. 2016. Batched Gaussian process bandit optimization via determinantal point processes. In *NeurIPS*.
- Keskar, N. S.; Mudigere, D.; Nocedal, J.; Smelyanskiy, M.; and Tang, P. T. P. 2016. On large-batch training for deep learning: Generalization gap and sharp minima. *arXiv preprint arXiv:1609.04836*.
- Krizhevsky, A.; Hinton, G.; et al. 2009. Learning multiple layers of features from tiny images. *Tech Report*.
- Li, H.; Xu, Z.; Taylor, G.; Studer, C.; and Goldstein, T. 2017. Visualizing the loss landscape of neural nets. *arXiv preprint arXiv:1712.09913*.
- Li, L.; Khodak, M.; Balcan, M.-F.; and Talwalkar, A. 2021. Geometry-aware gradient algorithms for neural architecture search. In *ICLR*.
- Li, L.-J.; and Fei-Fei, L. 2007. What, where and who? Classifying events by scene and object recognition. In *ICCV*.
- Lim, S.; Kim, I.; Kim, T.; Kim, C.; and Kim, S. 2019. Fast autoaugment. In *NeurIPS*.
- Lin, C.; Guo, M.; Li, C.; Yuan, X.; Wu, W.; Yan, J.; Lin, D.; and Ouyang, W. 2019. Online hyper-parameter learning for auto-augmentation strategy. In *CVPR*.
- Liu, H.; Simonyan, K.; and Yang, Y. 2019. DARTS: Differentiable architecture search. In *ICLR*.
- Lorraine, J.; Vicol, P.; and Duvenaud, D. 2020. Optimizing millions of hyperparameters by implicit differentiation. In *International Conference on Artificial Intelligence and Statistics*.
- Lu, Z.; Whalen, I.; Boddeti, V.; Dhebar, Y.; Deb, K.; Goodman, E.; and Banzhaf, W. 2019. Nsga-net: neural architecture search using multi-objective genetic algorithm. In *Proceedings of the Genetic and Evolutionary Computation Conference*, 419–427.

- MacKay, M.; Vicol, P.; Lorraine, J.; Duvenaud, D.; and Grosse, R. 2019. Self-tuning networks: Bilevel optimization of hyperparameters using structured best-response functions. *arXiv preprint arXiv:1903.03088*.
- Maclaurin, D.; Duvenaud, D.; and Adams, R. 2015. Gradient-based hyperparameter optimization through reversible learning. In *ICML*.
- Maddison, C. J.; Mnih, A.; and Teh, Y. W. 2016. The concrete distribution: A continuous relaxation of discrete random variables. *arXiv preprint arXiv:1611.00712*.
- Min, A. T. W.; Gupta, A.; and Ong, Y.-S. 2020. Generalizing Transfer Bayesian Optimization to Source-Target Heterogeneity. *IEEE Transactions on Automation Science and Engineering*.
- Mittal, G.; Liu, C.; Karianakis, N.; Fragoso, V.; Chen, M.; and Fu, Y. 2020. HyperSTAR: Task-aware hyperparameters for deep networks. In *CVPR*.
- Nekrasov, V.; Chen, H.; Shen, C.; and Reid, I. 2019. Fast neural architecture search of compact semantic segmentation models via auxiliary cells. In *CVPR*.
- Nilsback, M.-E.; and Zisserman, A. 2008. Automated flower classification over a large number of classes. In *Indian Conference on Computer Vision, Graphics & Image Processing*.
- Perrone, V.; Jenatton, R.; Seeger, M.; and Archambeau, C. 2018. Scalable hyperparameter transfer learning. In *International Conference on Neural Information Processing Systems*.
- Pham, H.; Guan, M.; Zoph, B.; Le, Q.; and Dean, J. 2018. Efficient neural architecture search via parameters sharing. In *ICML*.
- Quattoni, A.; and Torralba, A. 2009. Recognizing indoor scenes. In *CVPR*.
- Real, E.; Aggarwal, A.; Huang, Y.; and Le, Q. V. 2018. Regularized evolution for image classifier architecture search. *arXiv:1802.01548*.
- Ru, B.; Alvi, A. S.; Nguyen, V.; Osborne, M. A.; and Roberts, S. J. 2020. Bayesian optimisation over multiple continuous and categorical inputs. In *ICML*.
- Ru, B.; Esperança, P.; and Carlucci, F. 2020. Neural architecture generator optimization. In *NeurIPS*.
- Russakovsky, O.; Deng, J.; Su, H.; Krause, J.; Satheesh, S.; Ma, S.; Huang, Z.; Karpathy, A.; Khosla, A.; Bernstein, M.; et al. 2015. Imagenet large scale visual recognition challenge. *IJCV*.
- Sandler, M.; Howard, A.; Zhu, M.; Zhmoginov, A.; and Chen, L.-C. 2018. MobilenetV2: Inverted residuals and linear bottlenecks. In *CVPR*.
- Shaban, A.; Cheng, C.-A.; Hatch, N.; and Boots, B. 2019. Truncated back-propagation for bilevel optimization. In *International Conference on Artificial Intelligence and Statistics*.
- Swersky, K.; Snoek, J.; and Adams, R. P. 2013. Multi-task bayesian optimization. In *NeurIPS*.
- Tan, M.; and Le, Q. 2019. Efficientnet: Rethinking model scaling for convolutional neural networks. In *International Conference on Machine Learning*, 6105–6114. PMLR.
- Tibshirani, R. 1996. Regression shrinkage and selection via the lasso. *Journal of the Royal Statistical Society: Series B (Methodological)*, 58(1): 267–288.
- Wang, T.; Wang, K.; Cai, H.; Lin, J.; Liu, Z.; Wang, H.; Lin, Y.; and Han, S. 2020. APQ: Joint Search for Network Architecture, Pruning and Quantization Policy. In *CVPR*.
- Wei, L.; Xiao, A.; Xie, L.; Chen, X.; Zhang, X.; and Tian, Q. 2020. Circumventing Outliers of AutoAugment with Knowledge Distillation. *CoRR*, abs/2003.11342.
- Williams, R. J. 1992. Simple statistical gradient-following algorithms for connectionist reinforcement learning. *Machine Learning*, 8(3-4): 229–256.
- Wu, J.; Toscano-Palmerin, S.; Frazier, P. I.; and Wilson, A. G. 2019. Practical multi-fidelity Bayesian optimization for hyperparameter tuning. In *UAI*.
- Xie, L.; Chen, X.; Bi, K.; Wei, L.; Xu, Y.; Chen, Z.; Wang, L.; Xiao, A.; Chang, J.; Zhang, X.; and Tian, Q. 2020. Weight-Sharing Neural Architecture Search: A Battle to Shrink the Optimization Gap. *CoRR*, abs/2008.01475.
- Xie, S.; Zheng, H.; Liu, C.; and Lin, L. 2019. SNAS: Stochastic neural architecture search. In *ICLR*.
- Xu, H.; and Mannor, S. 2012. Robustness and generalization. *Machine learning*, 86(3): 391–423.
- Xu, Y.; Xie, L.; Zhang, X.; Chen, X.; Qi, G.-J.; Tian, Q.; and Xiong, H. 2020. PC-DARTS: Partial channel connections for memory-efficient architecture search. In *ICLR*.
- Yang, A.; Esperança, P. M.; and Carlucci, F. M. 2019. NAS evaluation is frustratingly hard. *arXiv preprint arXiv:1912.12522*.
- Yang, Y.; Li, H.; You, S.; Wang, F.; Qian, C.; and Lin, Z. 2020. ISTA-NAS: Efficient and consistent neural architecture search by sparse coding. *arXiv preprint arXiv:2010.06176*.
- Yao, L.; Xu, H.; Zhang, W.; Liang, X.; and Li, Z. 2020. SM-NAS: structural-to-modular neural architecture search for object detection. In *AAAI*.
- Zela, A.; Klein, A.; Falkner, S.; and Hutter, F. 2018. Towards automated deep learning: Efficient joint neural architecture and hyperparameter search. *arXiv preprint arXiv:1807.06906*.
- Zhang, X.; Wang, Q.; Zhang, J.; and Zhong, Z. 2020. Adversarial autoaugment. *ICLR*.
- Zhou, H.; Yang, M.; Wang, J.; and Pan, W. 2019. Bayesnas: A bayesian approach for neural architecture search. In *ICML*.
- Zoph, B.; and Le, Q. 2017. Neural architecture search with reinforcement learning. In *ICLR*.

Appendix

Detailed Experimental Settings

Search Space

(1) **Automated DA** Following (Ho et al. 2019), we consider 14 different operations for data augmentation, including:

● AutoContrast ● Equalize ● Rotate ● Posterize ● Solarize ● Color ● Contrast ● Brightness ● Sharpness ● Shear X ● Shear Y ● Translate X ● Translate Y ● Identity.

The magnitude ranging from 0 to 10 of each operation is randomly sampled from a uniform distribution. At each time, two operations would be sampled according to τ and would be successively applied to each sample.

(2) **NAS** Following (Liu, Simonyan, and Yang 2019), we consider the cell-based search space, which regards the whole architecture as a stack of similar cells. Each cell consists of a fixed number of nodes and our model tries to find the best operation combination between different nodes. One difference worth mentioning is that in contrast to DARTS (Liu, Simonyan, and Yang 2019) which has 8 different operations between two nodes, we adopt the setting in (Yang et al. 2020) which only considers 7 different operation options between two nodes including:

● 3×3 Separable Convolutions ● 5×5 Separable Convolutions ● 3×3 Dilated Separable Convolutions ● 5×5 Dilated Separable Convolutions ● 3×3 Max Pooling ● 3×3 Average Pooling ● Identity.

(3) **HPO** In our model, we consider both the L2 regularization (i.e., weight decay) and the learning rate in the experiments involving the HPO.

Setting These experiments are run on NVIDIA V100 under PyTorch-1.3.0 and python3.6. We adopt the hyperparameter setting in (Liu, Simonyan, and Yang 2019). As to the two-stage NAS, for experiments with CIFAR10, CIFAR100, SPORT8, MIT67, and FLOWERS102 during the search phase, the initial channel number and the cell number of the architecture are respectively 16 and 8. During the retraining/tuning phase, the final channel number and the cell number of the architecture are respectively 36 and 20. For experiments with ImageNet, the initial channel number of the architecture is 48 and the cell number of the architecture is 4. During the final retraining/tuning phase, the final channel number and the cell number of the architecture are respectively 48 and 14.

As to the one-stage NAS, for experiments with CIFAR10, CIFAR100, SPORT8, MIT67, and FLOWERS102, the channel number and the cell number of the architecture are respectively 36 and 20. For experiments with ImageNet, the channel number and the cell number of the architecture are respectively 48 and 14.

Ablation Study of Data Augmentation

Besides, we conduct an ablation study on the effect of doing both DA and HPO by comparing sequential DA+HPA and joint-optimization DA+HPO against several previous DA algorithms including one baseline method, Fast Autoaugment (FAA) (Lim et al. 2019), Population-Based Augment (PBA) (Ho et al. 2019) and RandAugment(RA) (Cubuk et al. 2020).

The **Baseline** method with CIFAR10 and CIFAR100 will standardize the data, use horizontal flips with 50% probability, add zero paddings, implement random crops, and finally apply cutout with 16×16 pixels. The **Sequential DA+HP** first applies DA strategy optimization to find a fixed DA strategy, then re-initializes the parameter weights and tunes them with HPO. The **Joint-optimization DA+HP** simultaneously conducts DA strategy optimization, HPO, and parameters weights tuning. From Table 4, we can learn two insights. Firstly, compared with previous data augmentation algorithms, the proposed DA can achieve similar performance with low computational requests. Secondly, the additional consideration of HPO can improve over DA-only approaches, and again joint-optimization of both components performs better than sequential-optimization of them.

Analysis of searched architectures

Temporal stability of searched architecture

The architectures discovered by Sequential DHA and DHA on Flowers102 are shown in Fig. 4. Differences between the two found architectures reveal two insights. Firstly, architecture found by Sequential DHA includes almost all kinds of operations and each of them occupies a similar portion. While, for the architecture found by DHA, few operations will occupy relatively large portion. Secondly, for the architecture found by DHA, operation with learn-able weights, e.g., 3×3 Dilated Separable Convolutions, will play an important role, while for the architecture found by Sequential DHA, non-weights operation, e.g., Identity will also play an essential actor. With the non-weights operation, during the search stage, it can easily lead to over-fitting, which prevents the algorithm to explore more possible operations. **All necessary code for re-implementing DHA on Cifar10 is provided in the supplementary material.**

Table 4: Top-1 Accuracy (%) comparison of different baseline networks with different DA optimization and HPO strategies on CIFAR10 and CIFAR100. Listed algorithms includes Baseline algorithm, FAA, PBA, RA, Sequential DA+HP and Joint-optimization DA+HP.

Strategy	CIFAR10		CIFAR100	
	Wide-ResNet-28-10	Wide-ResNet-40-2	Wide-ResNet-28-10	Wide-ResNet-40-2
Baseline	96.1	94.7	81.2	74.0
FAA	97.3	96.4	82.9	79.3
PBA	97.4	-	83.3	-
RA	97.3	-	83.3	-
Sequential DA+HPO	97.5	96.4	83.5	79.5
Joint-optimization DA+HPO	98.0	96.7	84.1	80.6

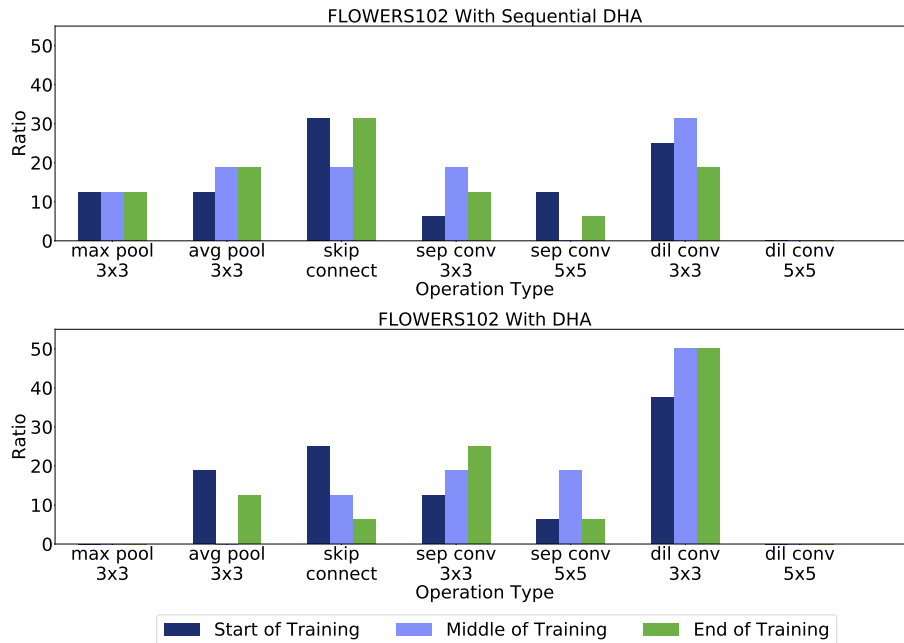


Figure 4: Temporal evolution of search architecture.